Probing cell shape regulation with patterned substratum: requirement of myosin II-mediated contractility†‡

Christopher C. Mader,§[ab] Edward H. Hinchcliffe[b] and Yu-li Wang*[a]

Received 9th May 2006, Accepted 30th August 2006
First published as an Advance Article on the web 20th September 2006
DOI: 10.1039/b606590b

Adherent cells cultured on flat, homogeneous surfaces typically maintain an intact cell body with a polygonal or fan shape, despite active migration and strong mechanical interactions with the substratum. We hypothesized that, in addition to the constraint of the surface membrane, an active mechanism may be involved in maintaining the shape and integrity of the cell body particularly where cells encounter complex topographic patterns of guidance cues. To detect if there is a mechanism that constrains cell shape, we plated NIH 3T3 fibroblasts on ring-patterned substrata 8–17.5 microns in width and 53–133 microns in outer diameter. Untreated cells have a limited angular span, encompassing an average of 108 degrees around the ring, even though these cells were able to cover a much larger surface when plated on flat surfaces of the same material. Treatment of 3T3 cells with a myosin II inhibitor, blebbistatin, induced a striking increase in the bending ability, causing cells to cover more than 60% of the ring. Inhibition of the Rho-dependent kinase with Y-27632 caused a similar but smaller increase in the angular span. Our results suggest that cell shape is controlled not only by the passive constraint of the surface membrane but also by an active mechanism driven by myosin II-mediated contractility under the regulation of Rho-dependent kinase. The inward surface tension-like forces allow the cell to maintain its integrity while navigating through complex physiological environments.

Introduction

Maintenance of shape and integrity represents a fundamental requirement of animal cells. Except during cell division, it is critical for a cell to keep its motile parts from separating from the body, while allowing the cell to move and change shape in response to complex chemical, physical, and topographical cues. It also appears critical that cell shape be constrained such that chemical or mechanical interactions among subcellular regions are not compromised by excessive distance or curvature.[1] In exceptional cases such as neurons, special structural and transport mechanisms have been developed to compensate for the unusual shape or dimension.[2]

Supported by classic studies with erythrocytes,[3] it is widely accepted that the plasma membrane and associated actin cytoskeleton play a key role in maintaining the cell shape. The involvement of actin is further supported by the drastic branching and fragmentation of cells upon treatment with disrupting agents such as cytochalasins.[4] However, exactly how the actin cytoskeleton controls cell shape is not clear. At the simplest level, the actin cytoskeleton may function merely as a structural support, conferring some rigidity and tenacity to an otherwise soft and labile lipid bilayer. This stabilization mechanism may allow cells to take any shape as long as the total surface area does not exceed that allowed by the cytoskeleton. Additional constraints to cell shape may be imposed by the elasticity of the cytoskeleton, which prevents cells from drastic bending by raising the potential energy. Alternative to these passive mechanisms is an active, motor-dependent activity that maintains cell shape by pushing or pulling the membrane. These forces may control not only the extent of extension but also membrane curvature throughout the cell. While direct evidence is lacking, this active mechanism is supported by the ability of a cell to retract its trailing end during migration,[5] and to minimize bending as demonstrated by the preferential longitudinal alignment on cylindrical surfaces.[6,7]

Previous studies have used patterned substrata to probe the responses of cells to different shapes imposed by adhesive reactions.[8,9] These results demonstrated the ability of cells to

[a]*Department of Physiology, University of Massachusetts Medical School, Worcester, Massachusetts 01655, USA. E-mail: yuli.wang@umassmed.edu*
[b]*Department of Biological Sciences, University of Notre Dame, Notre Dame, Indiana 46556*

† This paper is part of a *Soft Matter* themed issue on Proteins and Cells at Functional Interfaces. Guest editor: Joachim Spatz.

‡ Electronic supplementary information (ESI) available: Movie 1. Time-lapse movie of fibroblasts on ring substrata. NIH 3T3 cells plated on ring substrata were imaged after the cells were allowed to adhere for 5 hours. Images were acquired every 300 seconds and movie playback is at 6 frames per second. Movie 2. Time-lapse movie of fibroblasts on ring substrata treated with a myosin inhibitor. NIH 3T3 cells were plated on ring substrata then treated with 100 μM blebbistatin. Images were acquired every 300 seconds and movie playback is at 6 frames per second. Movie 3. Time-lapse movie of fibroblasts on ring substrata treated with an inhibitor against Rho-dependent kinase. NIH 3T3 cells were plated on ring substrata then treated with 20 μM Y-27632. Images were acquired every 300 seconds and movie playback is at 6 frames per second. Movie 4. Time-lapse movie of myosin IIB knockout fibroblasts on ring substrata. Fibroblasts from mice deficient in myosin IIB were plated on ring substrata. Images were acquired every 300 seconds and movie playback is at 6 frames per second. See DOI: 10.1039/b606590b

§ *Current address*: Department of Molecular Biophysics and Biochemistry, Yale University, New Haven, Connecticut 06510.

adapt to square and circular shapes, and to straddle multiple adhesive regions within certain distances. However, the relatively simple geometric patterns imposed only limited strain on cell shape and dimension. To probe the extent of shape control, it is necessary to challenge cells with a more demanding geometry. To this end we have developed a novel patterned substratum consisting of micron-sized adhesive rings isolated by non-adhesive polyacrylamide barriers. We found that fibroblasts normally resist bending around the rings but can be induced to do so by reducing the contractile forces generated by the actomyosin system. Our results suggest that adherent cells use a myosin-dependent, surface tension-like mechanism to maintain their integrity, by limiting extreme deformation and/or dimension.

Materials and methods

Preparation and characterization of ring substrata

Ring substrata were prepared by coating coverslips with a non-adhesive polymer (layer 1) followed by depositing ring-patterned adhesive polymers with photolithography (layer 2) and grafting additional polymers on non-adhesive regions (layer 3) to create a three dimensional barrier (Fig. 1C). The ring pattern was chosen over those with acute angles because it maintains a constant geometry in different subregions and allows simple assessment of cell shape based on the angular span. Layer 1, composed of polyacrylamide, was prepared from acrylamide (40% stock w/v; Bio-Rad Laboratories, Hercules, CA) and *N*,*N*-methylene-bis-acrylamide (BIS, 2% stock w/v; Bio-Rad) at a final concentration of 5% acrylamide and 0.1% BIS. The polymer was covalently attached to activated 45 mm round coverslips as described previously,[10,11] and allowed to air dry forming a thin film. Layer 2 consisted of SU-8 photoresist (MicroChem, Newton, MA), applied on top of layer 1 by spin coating. The surface was exposed to UV from an XBO-150 arc lamp through a ring-patterned mask for 1 minute and baked at 95 °C for 2 minutes. Exposed surface was developed with the SU-8 developer (MicroChem) for 1 minute, rinsed with 95% ethanol, and allowed to air dry. Layer 3 was prepared from acrylamide as for layer 1 except for the omission of BIS to allow the formation of non-crosslinked linear polymers, by inverting the substratum over 100 μl of activated acrylamide solution on a glass surface coated with SigmaCoat (Sigma-Aldrich Chemical, St. Louis, MO). As a result a jungle of linear polymers was grafted onto the dried layer of polyacrylamide (layer 1) but not onto areas covered by SU-8, forming three-dimensional barriers for cell migration.

A coverslip carrying ring substrata was glued onto the bottom of a 60 mm Petri dish with a 35 mm hole, to form a culture chamber. The surface was incubated with 1 mg ml^{-1} fibronectin in PBS (Sigma) for 1 hour at 37 °C before use. The thickness of the grafted polyacrylamide in layer 3 was estimated by observing fluorescent beads (1.0 μm Fluospheres, Molecular Probes, Eugene, OR) embedded in the polymers with a fluorescence microscope equipped with a calibrated focusing knob.

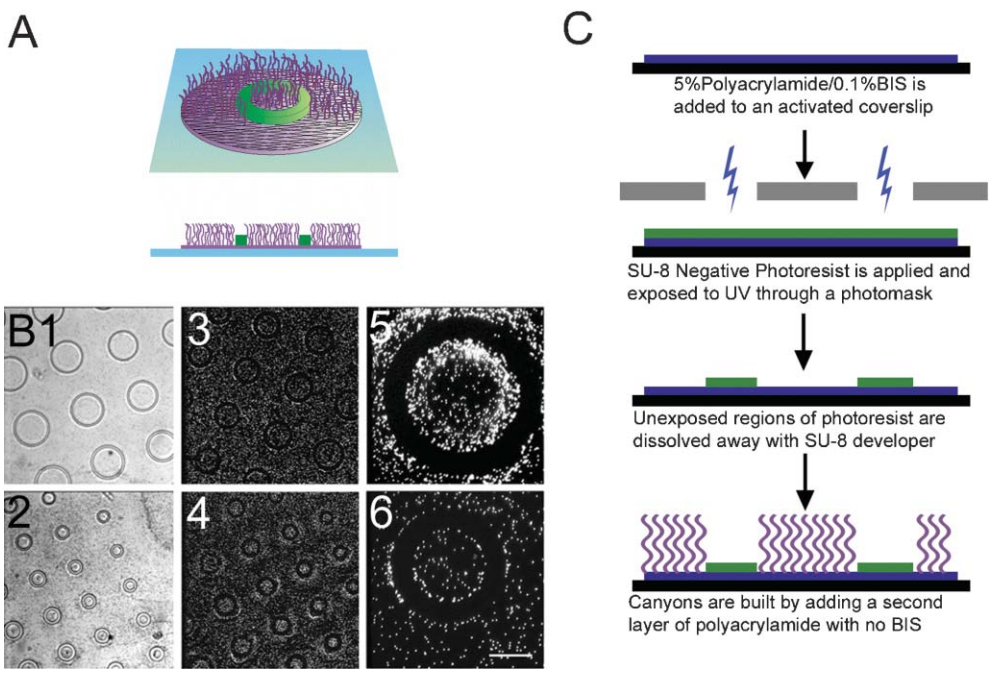

Fig. 1 Diagram (A) and fluorescence images (B) of the ring substratum. Ring substrata are constructed by covering the coverslip surface (blue-green) with a thin layer of dried, crosslinked polyacrylamide (purple), followed by ring patterned photoresist (green). The surface of polyacrylamide is then grafted with a layer of non-crosslinked polyacrylamide (curved lines). Phase contrast (B1 and B2) and fluorescence (B3–B6) images show the rings and fluorescent beads embedded in the bushes of non-crosslinked polyacrylamide surrounding the rings. (C) A schematic flowchart displaying the steps in preparing the ring substratum. A layer of crosslinked polyacrylamide is first dried onto a coverslip (step 1). The surface is spin-coated with the SU-8 photoresist and exposed to UV through a photomask (step 2). Exposed SU-8 is then removed with a developer, leaving a pattern of rings (step 3). A second layer of linear polyacrylamide is grafted onto the first layer, forming three-dimensional barriers (step 4). Bar, 60 μm (B1–B4), 40 μm (B5–B6).

Cell culture and microscopy

NIH 3T3 cells were cultured in DME (Sigma-Aldrich Chemical, St. Louis, MO), supplemented with 10% donor calf serum (JHR Biosciences, Lenexa, KS), 2 mM L-glutamine, 50 μg ml^{-1} streptomycin, and 50 U ml^{-1} penicillin (Gibco-BRL, Rockville, Maryland). Phase contrast images of cells on the substratum and fluorescence images of substrata embedded beads were recorded with a Zeiss Axiovert 200 M, Aviovert 100, Axiovert IM microscope (Carl Zeiss, Thornwood, NY), or a Leica DM IRBE microscope (Leica Microsystems, Bonnockburn, IL), equipped with a custom stage incubator and a 40× 0.70 NA Apochromat dry objective lens or a 20× Fluotar dry objective lens. A 41002c-UV filter set (Chroma Technologies, Brattleboro, VT) was used to observe the red fluorescent beads. Fluorescence images were collected using a cooled CCD camera with an EEV57 back-illuminated chip and an ST133 controller (Princeton Instruments, Trenton, NJ). Phase contrast images were gathered using either the cooled CCD camera or a 12V1-EX surveillance video camera (Mintron, Taipei, Taiwan). Live cells were followed at an interval of 180–300 seconds for 10–12 hours.

Cells were fixed and stained with rhodamine phalloidin following the supplier's protocol (Molecular Probes). Confocal images of actin filaments were collected using a 40× Plan Apochromat N.A.1.2 oil immersion lens on a Leica TCS SP2 scanning laser confocal mounted on a DM IRE2 microscope (Leica Microsystems). Maximum-intensity projection images were constructed from 20 images taken as a *Z*-series, and color-coded based on the distance from the substratum using Leica confocal software.

NIH3T3 fibroblasts were treated 5 hours after plating on the substratum with 100 μM blebbistatin (Toronto Research, Toronto, Canada), 20 μM Y-27632 (Welfide Corp., Osaka, Japan), 10 μM ML-7 (Calbiochem, San Diego, CA), or 10 μM nocodazole (Sigma) and imaged for 10–12 hours. Myosin IIB knockout fibroblasts were prepared as described previously.[12]

Image analysis

Measurements of angular span were made using custom software, which took a user defined tip and tail of a cell and computed the fraction of the ring circumference spanned by the cell. The analyses were based on the maximal angle for each cell over 10–12 hours. Measurements were confined to rings that ranged between 53–133 μm in diameter and 8–17.5 μm in width, since larger rings may exceed the spreading limit of cells while smaller rings were unable to keep the cells from covering the central region. In addition measurements were only taken of cells that were either solitary on the ring or were making no contact with other cells.

Results

Fabrication and characterization of ring substrata

To probe the mechanism regulating cell shape, we developed a simple, novel microfabrication technique for generating patterns of adhesive surfaces. We showed previously that cultured fibroblasts adhere poorly to polyacrylamide surfaces.[13] In contrast, cells adhered readily to a cured SU-8 photoresist surface coated with fibronectin (described later). Therefore, patterns of adhesiveness may be easily generated by applying SU-8 onto dried polyacrylamide, followed by UV exposure through a photomask to induce patterned cross-linkage of SU-8 and removal of unexposed SU-8 with a solvent developer (Fig. 1). To prevent cells from spreading across the center of rings, a second, hydrated polyacrylamide layer was grafted on top of the dried polyacrylamide surface within and around the adhesive rings to create a three-dimensional, non-adhesive barrier (Fig. 1).

The height of the photoresist ring was estimated to be 5 μm based on manufacturer's specifications and verified using a calibrated focusing motor on the microscope (Fig. 1A). To visualize the hydrated polyacrylamide barrier, red fluorescent beads 1 μm in diameter were added to the acrylamide solution prior to polymerization. As shown in Fig. 1B, the adhesive rings were devoid of the beads, but were isolated from one another by the dense bead-containing polyacrylamide barrier. Using a calibrated microscope focusing motor to measure the vertical distance of beads near the top and bottom of the barrier, the height of the barrier was estimated to be 10 μm. Taking into account the height of 5 μm for the photoresist, the barrier was estimated to stand 5 μm above the surface of the ring.

Confinement of cell shape by ring substrata

To determine if the surface of the photoresist was suitable for cell culture, NIH 3T3 fibroblasts were seeded on glass coverslips coated with photoresist followed by fibronectin. As for cells on fibronectin-coated glass, these cells adhered and spread rapidly, reaching a steady state within 3 hours. The spreading area was statistically indistinguishable between fibroblasts plated on glass and SU-8 (2953 ± 637 μm^2 $n = 13$ *versus* 3625 ± 476 μm^2 $n = 14$; $p = 0.40$; Fig. 2E). In addition, cells on photoresist and on glass coverslips showed similar actin organization (Fig. 2B and D), migration and multiplication (data not shown).

Experiments were performed with rings 8–17.5 μm in width and 53–133 μm in diameter. The total surface area ranged between 1000 and 4700 μm^2. As NIH 3T3 cells plated on fibronectin-coated glass coverslips spread to an average of 2953 ± 637 μm^2 ($n = 13$; Fig. 2E), cells plated on small rings are expected to be able to cover the entire surface of small rings and 50% of the surface of large rings, if spreading area were the only constraint.

When plated on ring substrates, most (85%) cells remained within the ring area 5 hours after plating (Fig. 3B). Short bundles of actin filaments extending across the cell width were confined to a single plane of focus under confocal optics (Fig. 3B, Fig. 4B and D). The remaining cells that spanned the central region assembled long, arching actin bundles that extended across the cell body and terminated at the ring (Fig. 4A and C). These results suggest that the ring substratum provided effective constraints for the cell shape.

Limited angular span of cells within ring substrata

Once adhered to the ring substratum, 3T3 cells began to expand and migrate around the ring within 15 minutes.

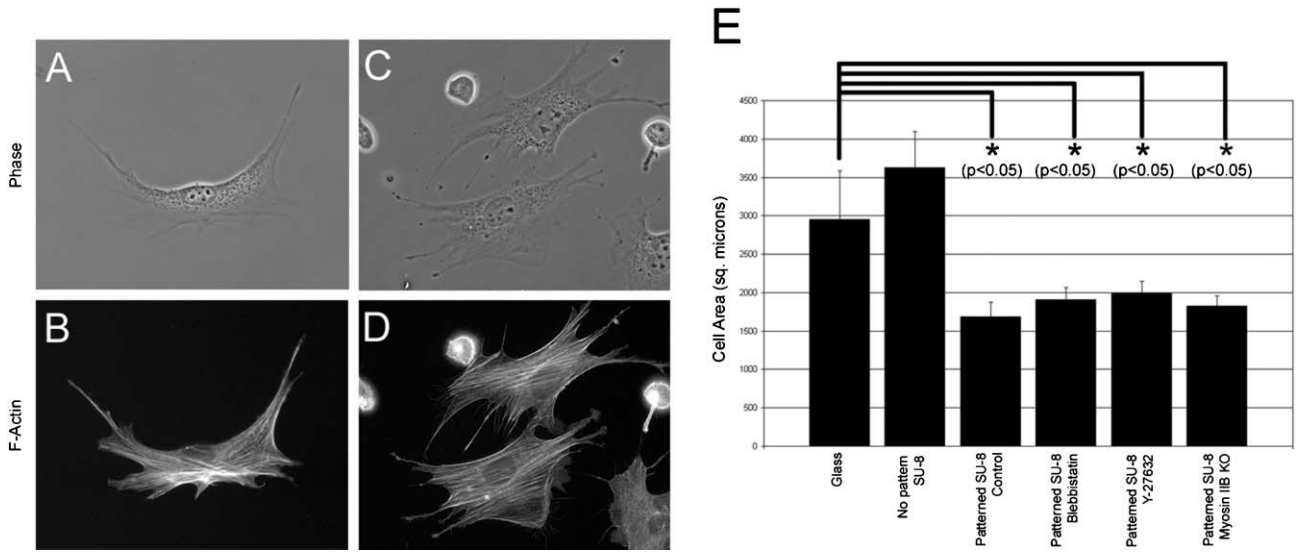

Fig. 2 Morphology, actin organization, and spreading of NIH 3T3 cells on fibronectin-coated glass (A, B) or non-patterned SU-8 substrata (C, D). Phase contrast (A, C) shows normal morphology on both surfaces. Corresponding images of rhodamine phalloidin staining show similar stress fiber organizations (B, D). (E) Analysis of cell area under different plating conditions and pharmacological treatments indicate no significant difference ($p > 0.05$) in spreading between glass (2953 $\pm$ 637 μm^2, $n = 13$) and non-patterned SU-8 (3625 $\pm$ 476 μm^2, $n = 14$). Cells plated on the ring substratum show a significant ($p < 0.05$; 1685.6 $\pm$ 188.8 μm^2 $n = 18$) decrease in spreading area relative to cells plated on unpatterened SU-8 or glass. However neither treatment with myosin inhibitors (1906.3 $\pm$ 159.1 μm^2 $n = 11$ in blebbistatin and 1987.5 $\pm$ 160.7 μm^2 $n = 8$ in Y-27632) nor ablation of myosin IIB (1827.1 $\pm$ 132.5 μm^2 $n = 13$) caused further significant change in spreading area on ring substrata (bar = 40 μm (A–D)).

However, the cells were never able to bend beyond about 25% of the ring (Fig. 3B). Measurements of maximal angular span over a period of 4 hours for each cell yielded an average of 108 $\pm$ 6 degrees ($n = 18$; Fig. 5 and Fig. 6A). Furthermore, the spreading area remained significantly smaller (1685 $\pm$ 189 μm^2, $n = 18$) than that of cells plated on either fibronectin-coated glass ($p < 0.04$) or non-patterened SU-8 ($p < 0.001$). Since the spreading area on non-patterned surfaces was sufficient to cover at least half of the ring area (Fig. 2B), the limited angular span cannot be explained by the availability of adhesive surface. Also of interest is that the angular span was independent of the ring diameter, as indicated by the shallow slope of the response of angular span to ring diameter and a low covariance between the two (0.077; Fig. 6B).

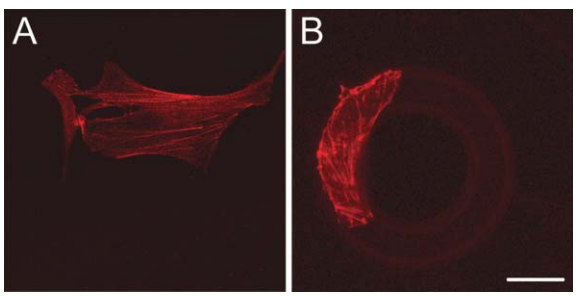

Fig. 3 Organization of actin filaments in NIH 3T3 cells plated on non-patterned (A) or ring patterned (B) substrata. Staining with fluorescent phalloidin shows similar stress fibers in both cases, except that the cell on the ring substratum has a more compact shape and shorter actin bundles. Images are average intensity projections from a *Z*-stack of 10 optical sections at a distance of 0.5 μm from one another. Bar, 20 μm.

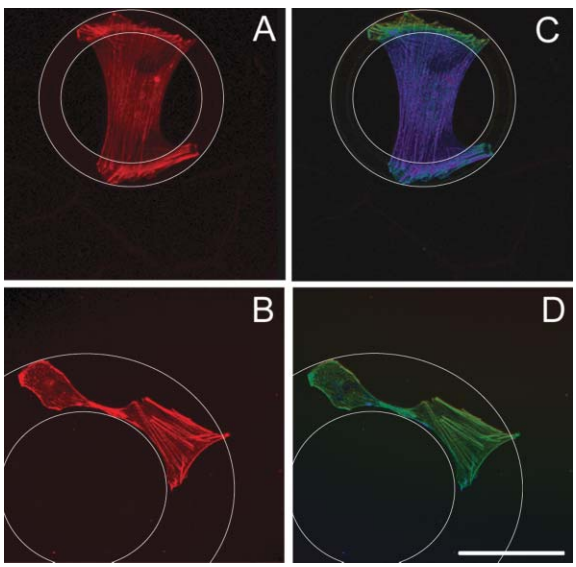

Fig. 4 Maximum intensity projection (A, B) and focal plane analysis (C, D) of actin filament bundles in 3T3 cells. 3T3 fibroblasts are stained with rhodamine phalloidin and *Z*-stacks of fluorescence images collected with a laser scanning confocal microscope. The stacks are shown either as a maximum intensity projection (A, B) or as superimposed images with different focal planes coded in different colors (C, D). Higher focal planes are coded in cold colors and lower focal planes in warm colors. In a small percentage of cells that cover the center region of the ring, stress fibers extend over the poly-acrylamide barrier in the center (blue, C) and terminate on the ring substratum at a lower focal plane (yellow and green, C). The majority of cells that stay within the ring are on a single focal plane and are more compact in shape (B, D). White outlines indicate the position of the ring. Bar, 40 μm.

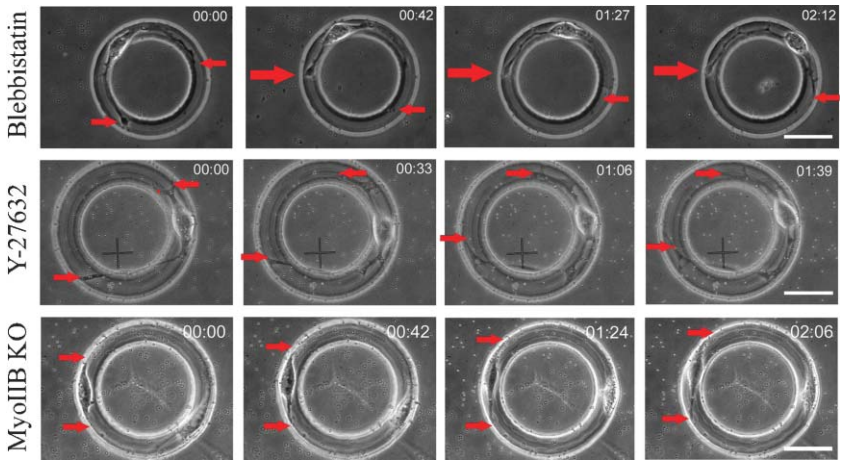

Fig. 5 Responses of cells on ring substrata to disruptions of myosin II. NIH 3T3 cells plated on ring substrata and treated with blebbistatin (top) or Y-27632 (middle) for up to 4 hours show an angular span that exceeds half of the ring (red arrows), while the cells remain motile. In contrast, fibroblasts in which myosin IIB has been genetically ablated span a much smaller fraction of the ring (bottom). Time 00:00 represents the time of treatment by profusion into the imaging chamber. Bar, 40 μm.

Involvement of myosin II in constraining the cell shape

To determine if contractile forces of the cytoskeleton contributed to cell shape control, we treated 3T3 cells with a variety of cytoskeletal inhibitors and measured their ability to bend around the ring substratum. Cells treated with blebbistatin, a potent inhibitor of the non-muscle myosin II ATPase,[14] exhibited a striking increase in the angular span from 108 degrees for control cells to 228 $\pm$ 18 degrees (n = 11; $p < 0.001$) Fig. 5 and Fig. 6A) but did not differ in cell area from controls (1906.3 $\pm$ 159.1 μm^2, n = 11, p = 0.77; Fig. 2E). In addition, the angular span became inversely dependent on ring diameter as indicated by a negative slope of -1.992 ± 0.4187 (r^2 = 0.7155) in least square linear regression and a covariance of -0.846 (Fig. 6B). Treatment with Y-27632, an inhibitor of Rho-dependent kinase and myosin II dependent traction forces,[15] caused a similar increase in angular span (average span of 138 $\pm$ 11 degrees, n = 8, $p < 0.04$; Fig. 5 and Fig. 6A), no change in cell area relative to controls (1987.5 $\pm$ 160.7 μm^2, n = 8 p = 0.99; Fig. 2E) and a similar inverse relationship between angular span and ring diameter (slope = -1.540 ± 0.4328, r^2 = 0.679 covariance = -0.824; Fig. 6B).

In contrast to the inhibition of myosin II by blebbistatin, genetic ablation of the myosin IIB isoform caused a mild shape defect and weak inhibition of traction forces.[12] These knock-out cells showed no detectable increase in the ability to bend around the ring substratum, but a slight decrease in angular span (average span = 91 $\pm$ 4 degrees; $p < 0.04$; n = 13; Fig. 5 and Fig. 6A), no change in cell area relative to controls (1827.1 $\pm$ 132.5 μm^2, n = 13, p = 0.53; Fig. 2E) and no correlation between ring diameter and angular span. Similarly, treatment with ML-7, an inhibitor of the myosin light chain kinase, caused neither inhibition of traction forces[15] nor an increase in cellular angular span (data not shown). Treatment of cells with the microtubule disassembly agent nocodazole had no effect on the angular span either (data not shown). Together, these results suggest that myosin II-dependent traction forces play a major role in regulating the shape of adherent cells.

Discussion

While flat, two-dimensional surfaces have been used extensively for cell biological studies, most cells *in vivo* are surrounded by an environment of complex topography. Three-dimensional "obstacle courses" serve as a useful experimental system for probing the ability of cells to adapt their shapes to the environment. In the present study, we developed a novel microfabrication technique to create adhesive, micron-sized rings isolated by non-adhesive polyacrylamide barriers. Observations of fibroblasts indicated a general resistance to bending, despite the compatibility of the ring surface with cell adhesion and the availability of spreading area. The results suggest that cell shape is regulated not only by the availability of membrane surface, but also by an active mechanism that limits the complexity of the shape. Moreover, through the use of pharmacological agents, we showed that this constraint in cell shape is driven by myosin II based contractility, and that the process is at least partially dependent on the Rho-dependent kinase and possibly the small GTPase Rho but is independent of the myosin light chain kinase.

Function of myosin II in cellular shape control

Myosin II, the mechanoenzyme responsible for muscle contraction,[16] is present in not only muscles but also in most non-muscle cells. Although myosin II-driven contraction has been investigated in detail in muscle cells, functions of non-muscle myosin are still poorly understood. For example, ablation of myosin II in *Dictyostelium* causes partial inhibition of cell migration but severe defects in the persistence of migration.[17] Similarly, inhibition of myosin II ATPase or the Rho-dependent kinase in cultured cells causes no significant inhibition of cell migration but irregular cell shapes,[18] suggesting that a primary function of myosin II may be the maintenance of cell shape and polarity.

Closely related to the above observations is the requirement of myosin II for the generation of traction forces, inward

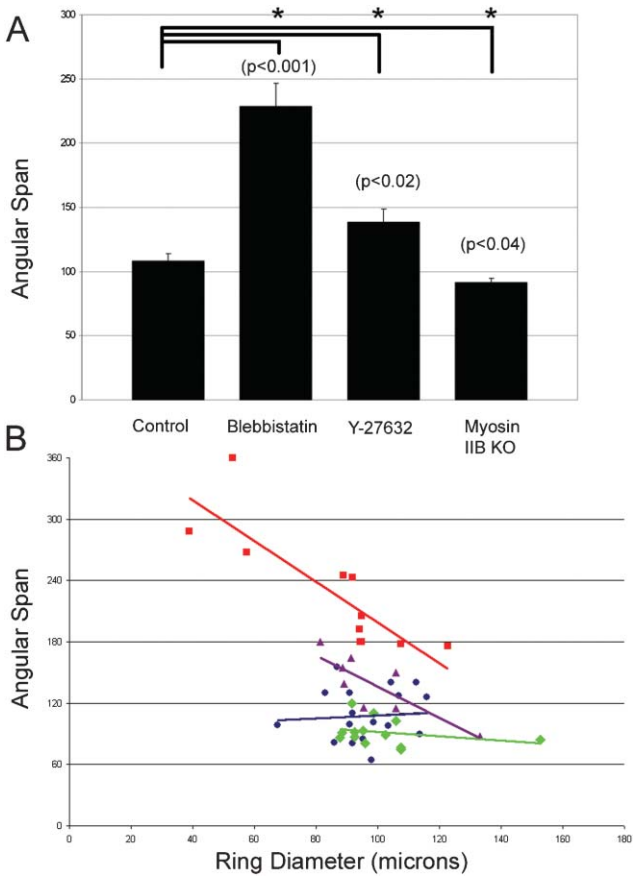

Fig. 6 Angular span of cells under various conditions. Bar graph (A) shows average angular span and SEM error bars. Student's t-test significance values are given relative to the control for each experimental condition with significant differences ($p < 0.05$) marked with an asterisk. The angular span increases following the inhibition of myosin II with blebbistatin and of Rho-dependent kinase with Y-27632 and decreases slightly in the myosin IIB knockout cells. Scatter plots with linear least square fit (B) indicate that cells treated with blebbistatin (red square) and Y-27632 (purple triangle) cover a progressively smaller angle as the diameter increases, as indicated by a negative slope of -1.992 ± 0.4187 for blebbistatin treated cells (red line) and -1.540 ± 0.4328 for Y-27632 treated cells (purple line). Control (blue circle, blue line) cells and myosin IIB knockout fibroblasts (green diamonds, green line) show a smaller angular span statistically independent of ring diameter.

mechanical forces detected underneath migrating cells.[15,19,20] As many rapidly migrating cells such as amoebae generate only very weak traction forces, these forces are unlikely to be directly responsible for cell migration. Their presence in highly adhesive cells such as fibroblasts suggests that these forces may be required to overcome conditions associated with strong adhesion, such as the retraction of an anchored tail, in order to maintain the cell shape. In addition, they may allow adhesive cells to detect shape and rigidity cues of the environment, and to orient their extensions accordingly.[21,22] Inward contractile forces may also maintain the cell shape by inhibiting lamellipodial extension in the lateral and posterior regions.

The simplest model to explain the present results is that inward contractile forces act on the cortex much like surface tension to liquid drops. As for surface tension, these forces cause the cell to resist bending and to take a compact form. For adherent cells, the shape at steady state is therefore determined by a balance of these inward forces against forces of substratum anchorage and protrusion. In the absence of the latter forces, cells round up much like liquid drops, a process seen following detachment from the substratum. Also consistent with the concept of surface tension, inhibition of myosin II generated inward contractile forces was found to promote the initial spreading of cells.[23]

The present results also shed light on the redundancy of different myosin isoforms and regulatory mechanisms. While global inhibition of myosin II activities caused a dramatic increase in angular span around the ring substrate, ablation of myosin IIB alone caused no detectable effect, suggesting that myosin IIA, the other myosin II isoform present in most non-muscle cells, performs either primary or redundant functions in generating the traction forces[12] and maintaining the cell shape. Similarly, inhibition of the myosin light chain kinase causes no effect on the shape constraint around the ring substrate, suggesting that either myosin light chain kinase performs unrelated functions or its inhibition is compensated by other kinases capable of phosphorylating the myosin regulatory light chain.

Functions of an active mechanism for cellular shape control

Cell migration is propelled by localized protrusions that respond to local chemical and physical signals.[24] However, without coordination, scattered protrusions may create a tug of war, inhibiting net cell migration and possibly causing cells to fragment. Global inward contractile activities keep the cell shape in a compact and intact form. For example, when faced with a complex environment of physical, topographical, and chemical cues, these forces may allow cells to respond in an unambiguous manner while maintaining their integrity. Regulation of cell shape is also important for the coordination of chemical events among different regions of the cell. Excessive linear dimensions or acute bending may impair the transport of molecules or organelles and the propagation of chemical signals. Using patterned substrata of different shapes and sizes, previous studies have demonstrated the profound effects of cell shape on signal transduction, cell cycle regulation, and apoptosis.[25,26]

Conclusion

In summary, the novel substratum design provides a powerful tool for the analysis of cellular shape constraints in response to two-dimensional topographic cues and/or three-dimensional obstructions in the environment. Combining this technology with molecular imaging should allow for a detailed analysis of intracellular events during shape adaptation. Moreover, in conjunction with high-throughput screens, patterned substrata should provide powerful means for characterizing genetic defects and for identifying new pharmacological agents that specifically affect cell shape regulation. The knowledge will lead to a better understanding of such processes *in vivo* as morphogenesis and wound healing, and *in vitro* as artificial tissue engineering.

Supplementary data

Movie 1. Time-lapse movie of fibroblasts on ring substrata. NIH 3T3 cells plated on ring substrata were imaged after the cells were allowed to adhere for 5 hours. Images were acquired every 300 seconds and movie playback is at 6 frames per second.

Movie 2. Time-lapse movie of fibroblasts on ring substrata treated with a myosin inhibitor. NIH 3T3 cells were plated on ring substrata then treated with 100 μM blebbistatin. Images were acquired every 300 seconds and movie playback is at 6 frames per second.

Movie 3. Time-lapse movie of fibroblasts on ring substrata treated with an inhibitor against Rho-dependent kinase. NIH 3T3 cells were plated on ring substrata then treated with 20 μM Y-27632. Images were acquired every 300 seconds and movie playback is at 6 frames per second.

Movie 4. Time-lapse movie of myosin IIB knockout fibroblasts on ring substrata. Fibroblasts from mouse deficient in myosin IIB were plated on ring substrata. Images were acquired every 300 seconds and movie playback is at 6 frames per second.

Acknowledgements

The authors wish to thank Dr. Al Crosby for the guidance in setting up bench-top photolithography. YLW is supported by NIH grant GM32476, CCM is supported by a NIH pre-doctoral training grant to Yale University, and EHH is supported by NIH Grant GM72754. EHH is a Research Scholar of the American Cancer Society.

References

1 A. J. Maniotis, C. S. Chen and D. E. Ingber, *Proc. Natl. Acad. Sci. U. S. A.*, 1997, **94**, 849–854.
2 B. Grafstein and D. S. Forman, *Physiol. Rev.*, 1980, **60**, 1167–1283.
3 V. Bennette, *Annu. Rev. Biochem.*, 1985, **54**, 273–304.
4 S. W. Tanenbaum, *Cytochalasins – Biochemical and Cell Biological Aspects*, Elsevier/North-Holland Biomedical Press, Amsterdam, 1978.
5 W. T. Chen, *J. Cell Biol.*, 1981, **90**, 187–200.
6 Y. A. Rovensky and V. I. Samoilov, *J. Cell Sci.*, 1994, **107**, 1255–1263.
7 E. M. Levina, L. V. Domnina, Y. A. Rovensky and J. M. Vasiliev, *Exp. Cell Res.*, 1996, **229**, 159–165.
8 C. S. Chen, E. Ostuni, G. M. Whiteside and D. E. Ingber, *Methods Mol. Biol.*, 2000, **139**, 209–219.
9 D. Lehnert, B. Wehrle-Haller, C. David, U. Weiland, C. Ballestrem, B. A. Imhof and M. Bastmeyer, *J. Cell Sci.*, 2004, **117**, 41–52.
10 Y.-L. Wang and R. J. Pelham, Jr., *Methods Enzymol.*, 1998, **298**, 489–496.
11 K. A. Beningo and Y.-L. Wang, *Trends Cell Biol.*, 2002, **12**, 79–84.
12 C.-M. Lo, D. B. Buxton, G. C. Chua, M. Dembo, R. S. Adelstein and Y.-L. Wang, *Mol. Biol. Cell*, 2004, **15**, 982–989.
13 R. J. Pelham, Jr. and Y.-L. Wang, *Proc. Natl. Acad. Sci. U. S. A.*, 1997, **94**, 13661–13665.
14 A. F. Straight, A. Cheung, J. Limouze, I. Chen, N. J. Westwood, J. R. Sellers and T. J. Mitchison, *Science*, 2003, **299**, 1743–1747.
15 K. A. Beningo, M. Dembo, Y.-L. Wang and H. Hosoya, *Arch. Biochem. Biophys.*, submitted.
16 H. E. Huxley, *Science*, 1969, **164**, 1356–1366.
17 D. Wessels, D. R. Soll, D. Knecht, W. F. Loomis, A. DeLozanne and J. A. Spudich, *Dev. Biol.*, 1998, **128**, 164–177.
18 G. Totsukawa, W. Wu, S. Yasuharu, D. J. Hartshorne, Y. Yamakita, S. Yamashiro and F. Matsumura, *J. Cell Biol.*, 2004, **164**, 427–439.
19 M. Dembo and Y.-L. Wang, *Biophys. J.*, 1999, **76**, 2307–2316.
20 S. Munevar, M. Dembo and Y.-L. Wang, *Biophys. J.*, 2001, **80**, 1744–1757.
21 K. K. Parker, A. L. Brock, C. Brangwynne, R. J. Mannix, N. Wang, E. Ostuni, N. A. Geisse, J. C. Adams, G. M. Whitesides and D. E. Ingber, *FASEB J.*, 2002, **16**, 1195–1204.
22 C.-M. Lo, H.-B. Wang, M. Dembo and Y.-L. Wang, *Biophys. J.*, 2000, **79**, 144–152.
23 T. Watatsuki, R. B. Wysolmerski and E. L. Elson, *J. Cell Sci.*, 2003, **116**, 1617–1625.
24 B. Geiger and A. Bershadsky, *Cell*, 2002, **110**, 139–142.
25 C. S. Chen, M. Mirksich, S. Huang, G. M. Whiteside and D. E. Ingber, *Science*, 1997, **276**, 1425–1428.
26 S. Huang, C. S. Chen and D. E. Ingber, *Mol. Biol. Cell*, 1998, **9**, 3179–3193.